Ice Dynamic Observation with Remote Sensing

1st Roberto Nardini
Italian Hydrographic Institute
DICCA, University of Genoa
Genova, Italy
roberto_nardini@marina.difesa.it

2nd Maurizio Demarte
Italian Hydrographic Institute
Genova, Italy
maurizio.demarte@marina.difesa.it

3th Filippo Britti
e-Geos
Roma, Italy
filippo.britti@e-geos.it

4th Bianca Federici
DICCA University of Genova
Genova, Italy
bianca.federici@unige.it

2025 IEEE International Workshop on Metrology for the Sea; Learning to Measure Sea Health Parameters (MetroSea) | 979-8-3315-7483-3/25/$31.00 ©2025 IEEE | DOI: 10.1109/MetroSea66681.2025.11245742

***Abstract*— During the High North hydro-oceanographic campaigns in the Arctic, one of the main challenges is planning the ship's routes to reach the areas of interest while ensuring the vessel's safety. During the High North24 campaign, recent internet connectivity technologies, even in remote areas such as the Arctic, enable rapid downloading of satellite data for on-board processing. Near-real-time information on ice distribution, concentration, drift speed and ice types were derived. Moreover, extensive observation, sampling, and ice characterization activities, using UAV acquisition, in situ collections and laboratory analysis, were carried out to enhance the understanding of this extreme environment that poses significant operational challenges.**

Keywords – Satellite monitoring, Sea Ice, Ice Drift, Ice Characterization, Polarimetry, Synthetic Aperture Radar (SAR).

I. Introduction

Since 2017, the High North program has carried out a series of hydro-oceanographic and marine geophysical campaigns in the Arctic waters surrounding the Svalbard Islands. These missions have been conducted aboard ITS Alliance, a vessel operated by the Italian Navy, which hosts a crew of 44 personnel in support of the embarked scientific team. The scientific contingent consists of a core group of hydrographers from the Italian Hydrographic Institute (IIM), with the collaboration of various national and international research institutions, including the National Research Council (CNR), the Italian National Agency for New Technologies, Energy and Sustainable Economic Development (ENEA), the National Institute of Geophysics and Volcanology (INGV), the Joint Research Centre (JRC-EU), the NATO Science and Technology Organization – Centre for Maritime Research and Experimentation (NATO-STO-CMRE), Sapienza University of Rome (UniRoma1), and the Italian National Institute of Health (ISS).

Key operations include acoustic seabed mapping with multibeam echosounders (MBES), complemented by geophysical and oceanographic data acquisition. These comprise sediment sampling, observational transects, meteorological and oceanographic measurements, bio-optical data, physical and biogeochemical parameters of the water column, assessments of marine pollution, and the sampling of macro-, micro-, and nanoplastics. The campaigns also involve the deployment of moorings as part of the SIOS (Svalbard Integrated Arctic Earth Observing System) international observation network.

Furthermore, the ARctic NAvigation with COSMO-SkyMed (ArNaCoSky) joint project between e-Geos (part of Telespazio S.p.A. and A.S.I.) and the Hydrographic Institute has been implemented. The project aims to provide an integrated sustainability assessment of Arctic navigation routes with the Italian COSMO-SkyMed constellation.

During the activities of the High North24 campaign (15 July–8 August 2024) (Fig. 1) an extensive effort was made in observing, monitoring, sampling, and characterizing the ice using various remote sensing techniques—including both satellite imagery and drone-based data acquisition—as well as in situ collections and laboratory analysis.

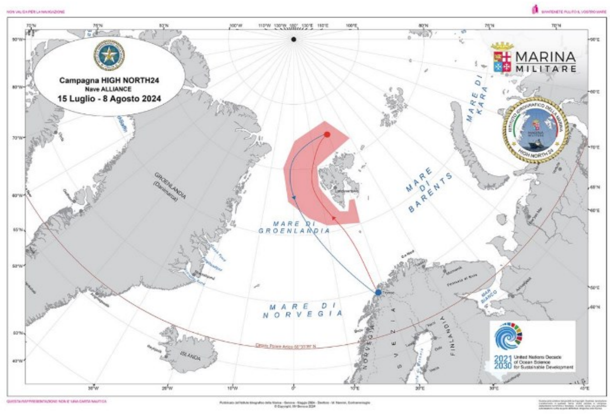

Fig. 1: Map showing the area covered by the High North24 campaign.

The main objectives of this study were:

1. Support for Arctic navigation – Several operations were conducted in areas with significant sea ice presence. Effective mission planning required near-real-time information on ice distribution, concentration, thickness and short-term drift forecasts, as compact ice represented a major constraint for safe navigation [1,2].
2. Environmental monitoring – Remote sensing techniques were employed to characterize sea ice, distinguishing among different ice types based on age and metamorphic state.
3. Acoustic propagation studies – Sea ice characteristics influence underwater acoustic transmission. Although direct measurements of subsurface ice morphology were not feasible during the campaign, surface classification could provide useful information for estimating sound speed profiles and potential effects on acoustic signal behavior.

979-8-3315-7483-3/25/$31.00 ©2025 IEEE

II. METHODOLOGY

A. Satellite observations

During the High North24 campaign, the position and dynamics of sea ice were analyzed daily using products provided by the Copernicus programme, the Earth Observation component of the European Space Agency managed by the European Commission. Specifically, data from the Sentinel-1 (SAR – C-Band – dual polarization) and Sentinel-2 (multispectral) missions were used, both freely downloadable from the public portal [3].

For most of the first phase of the campaign, Sentinel-1 SAR data proved essential for tracking ice position and assessing drift. SAR data have long been recognized as suitable for classifying and characterizing ice types based on their backscatter response [4,5]. One of the advantages of SAR data over multispectral data is that it is acquired daily, regardless of the presence of clouds or other atmospheric conditions [6]. Moreover, C-band SAR has traditionally been used to monitor sea ice extent, concentration, drift speed and ice type [7,8]. By overlaying images acquired at different times (Fig. 2), it was possible to detect both the speed and the direction of ice motion. In almost all cases, a consistent east/northeastward movement was observed, with an average speed of about 8-10 km per day. This dynamic is consistent with the wind data measured by the weather station onboard. The influence of currents cannot be ruled out, although it was not possible to analyze them during this period.

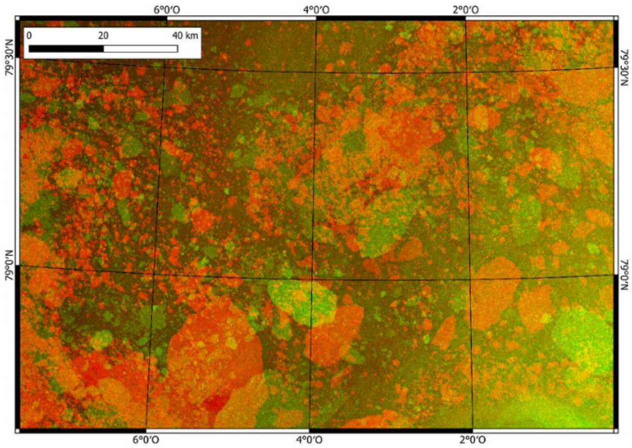

Fig. 2. Overlay of two Sentinel-1 images acquired at different times. The image taken on 19/07/24 at 07:53 is shown in green, and the position of the ice on 21/07/24 at 07:37 is shown in red. The eastward movement of the most recognizable ice blocks can be observed.

Unlike SAR, multispectral data from Sentinel-2 was strongly affected by the presence of clouds or fog, preventing data acquisition on certain days. Despite this, during the final phase of the campaign, thanks to favorable weather conditions, the data were crucial for on-board navigation planning, complementing the data acquired with COSMO-SkyMed, especially when Sentinel-1 data became scarce. Optical imagery has also enabled a clearer and more detailed observation of the presence of melt ponds on the ice [9]. Additionally, various band combinations highlighted the differences between ice and cloud cover (Fig. 3).

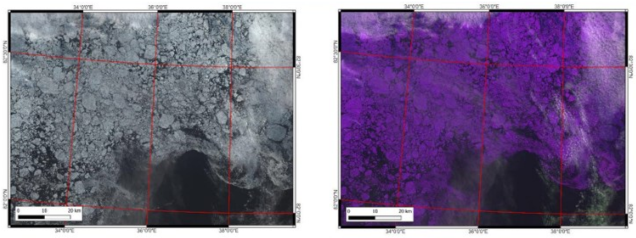

Fig. 3. Image taken by Sentinel-2B on 03/08/2024. On the left is the true-color image (RGB), while on the right is a false-color image (NIR, SWIR, Blue).

ArNaCoSky project was continued between 30/07/24 to 02/08/24, using the COSMO-SkyMed constellation. These satellites have a sun-synchronous, polar orbit (97.9° inclination) at an altitude of 619 km, with a revisit time of 16 days and an orbital period of 97.2 minutes. They are equipped with a Synthetic Aperture Radar (SAR) operating in the X-band, with a central frequency of 9.6 GHz, variable spatial resolution from 0.3m to 3m and 100m, and a swath ranging from 3 km x 7 km to 40 km x 40 km and 200 km x 200 km. SAR images are acquired in various combinations of spatial resolutions and polarizations: HH, HV, VV, VH.

During these activities, two locations per day were identified for image acquisition at the time of the satellite overpass, one in the morning and one in the afternoon. For each location, at least two images were acquired, one at low resolution with single polarization, and one at high resolution with multiple polarizations, using a combination of the following modes:

- First Generation CSK:
a) HR: 200 x 200 km, 1 polarization HH, and 100 m ground resolution.
b) WR: 100 x 150 km, 1 polarization HH, and 30 m ground resolution.
c) STR: 40 x 40 km, 1 polarization HH, and 3 m ground resolution.
- Second Generation CSG:
a) SC2: 200 x 200 km, 2 polarizations HH and HV, and 40 m ground resolution.
b) STR: 40 x 40 km, 2 polarizations HH and HV, and 3 m ground resolution (Fig. 4).
c) QPS: 15 x 40 km, 4 polarizations HH, HV, VV, VH, and 3 m ground resolution.

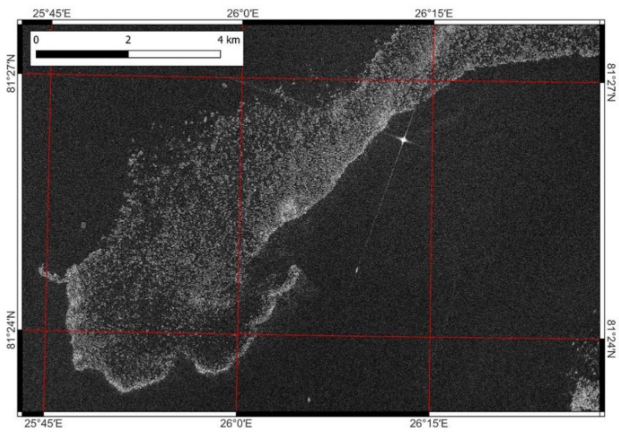

Fig. 4. Stripmap (STR) acquisition by COSMO-SkyMed of 01/08/2024. In the image is possible to see ITS Alliance with 3mx3m resolution with X-Band SAR.

B. Aerial observations

In addition to satellite remote sensing activities, drone flights were conducted during the High North24 campaign, generating orthomosaics (Fig. 5) to assess ice concentration in the area and 3D models to calculate the volume of exposed ice (Fig. 6). The data processing software used was Agisoft Metashape.

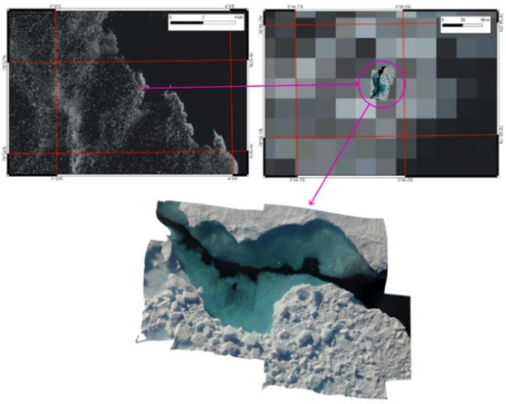

Fig. 5: Orthomosaic of the flight of 20/07/24. On the left, the area over a Sentinel 2 image, on the right the orthomosaic over the Sentinel 2 image, downside the orthomosaic.

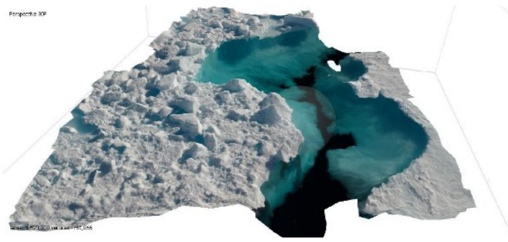

Fig. 6: 3D model of ice surface.

Two Uncrewed Aerial Vehicle (UAV) were used: a DJI Mavic 2 Enterprise Dual, equipped with a 12 MP camera and a 640x360 px thermal camera, and a DJI Mini 4 Pro with a 24MP CMOS wide-angle camera (Fig. 7).

Fig. 7: DJI Mavic 2 Enterprise Dual.

C. Resolution variability and operational implications

The three satellite systems provided complementary datasets, each with specific operational strengths and limitations (Table 1). Sentinel-1 ensured regular, weather-independent monitoring at medium resolution, making it suitable for large-scale drift tracking and navigation safety assessments. Sentinel-2, when available, enhanced ice-type discrimination and surface characterization thanks to its multispectral capabilities. COSMO-SkyMed, though limited in temporal coverage, offered the highest spatial resolution, enabling precise mapping of ice features and accurate geolocation of sampling sites.

TABLE I. OVERVIEW OF SATELLITE SENSOR SPECIFICATIONS

Satellite / Mode	Sentinel-1	Sentinel-2	COSMO-SkyMed CSK / CSG
Acquisition type	Radar (SAR)	Multispectral	Radar (SAR)
Frequency Band / Spectral Range	C-band (5.405 GHz)	VNIR & SWIR (443–2190 nm, 13 bands)	X-band (9.6 GHz)
Polarizations / Spectral Bands	HH, HV or VV, VH (up to 2 polarizations)	13 spectral bands (Coastal, Blue, Green, Red, 4 × Red-Edge, NIR, Narrow NIR, SWIR1, SWIR2)	HH, HV, VV, VH (up to 4 polarizations)
Ground Resolution	10–40 m	10–60 m	3–100 m
Main Advantages	All-weather, daily revisit, ice drift and type monitoring	Ice type discrimination, melt pond detection	Very high resolution, polarimetry capability
Limitations	Lower spatial detail compared to COSMO-SkyMed	Strongly affected by clouds/fog, limited availability	Only 5 days of data available during campaign period

D. Data integration and fusion approach

Due to the non-simultaneity of acquisitions from different sensors, full pixel-wise multi-sensor data fusion was not feasible: the rapid drift of sea ice meant that features could change position significantly between acquisition times. Consequently, during the initial phase of the campaign, image analysis was primarily based on visual interpretation, cross-referencing SAR, optical, and meteorological data to support navigation decisions.

In the final phase, semi-automatic classification algorithms were introduced, with COSMO-SkyMed polarimetric data used to explore ice-type discrimination. The validation of these classifications is still ongoing, based on laboratory analysis of in-situ ice samples collected during the ArNaCoSky period.

Where multi-sensor comparison was possible, two approaches were adopted:

1. **Equal-resolution comparison** – using imagery acquired at similar spatial resolutions to perform direct visual or algorithmic classification.
2. **Resolution matching for change detection** – degrading the higher-resolution image to match the lower-resolution dataset, then generating false-colour composites in which, for example, the green channel represented a band from the first acquisition and the red channel the same band from the later acquisition. This approach, combined with nearest-neighbour resampling to align grids, made it easier

to visually detect ice drift patterns over consecutive days (Fig. 2).

This operational methodology allowed each sensor to be exploited according to its strengths, ensuring continuous ice monitoring despite the constraints of weather conditions, satellite availability, and the dynamic nature of the Arctic ice environment.

E. Groundtruths

The capability of acquiring multiple polarizations per image with the second-generation COSMO satellites enables the application of polarimetry techniques, which relate the electromagnetic wave response to different material properties [10, 11, 12]. For this reason, this activity was coupled with *in situ* ice sampling in order to attempt classification of ice types based on satellite backscatter response.

A major challenge was the planning of satellite acquisitions and sampling points, as locations had to be selected and communicated almost 48 hours in advance. This introduced uncertainty, since the sea ice was highly dynamic: in some cases, the designated scene turned out to be either devoid of significant ice or entirely covered by compact ice, requiring last-minute repositioning of the sampling area.

In addition, the groundtruth phase presented specific operational limitations. The high-resolution dual- or quad-polarized COSMO-SkyMed images (40 × 40 km or 15 × 40 km) are acquired instantaneously over the full scene, whereas ship-based sampling requires at least one hour to collect three samples at distances of only a few hundred meters from each other. As a result, only a small number of samples, clustered in a restricted portion of the satellite footprint, could be collected for each acquisition, limiting the extent of validation across the image. A further difficulty arose from the mobility of sea ice: the drift, sometimes rapid, made it challenging to identify on the satellite image the exact floe from which the samples had been taken. Even with a spatial resolution of 3 m, linking a single pixel to quantitative laboratory measurements proved problematic. To mitigate this limitation, whenever wind and visibility conditions allowed, drone-based data were integrated with the sampling sessions. UAV orthophotos and 3D reconstructions provided additional detail on the shape and position of the floes, although their operational use was constrained by low temperatures and harsh environmental conditions.

Despite these constraints, the ArNaCoSky activity successfully concluded on 03/08/2024, when ITS *Alliance* managed to reach a latitude of 82° N, also thanks to the information derived from this project (Fig. 8).

The study involved multiple sampling sessions in which different ice and snow pieces were analyzed to assess variations in their physical properties, and water from melt ponds was collected for salinity measurements with a CTD probe in laboratory conditions. A total of 22 ice samples and 2 water samples from melt ponds were acquired (Fig. 9).

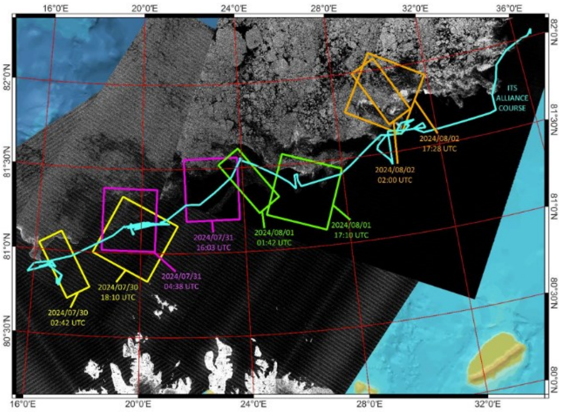

Fig. 8: ITS Alliance course from 30/07/2024 to 02/08/2024 overlapping with the footprints of the 8 high-resolution COSMO-SkyMed images.

Fig. 9: Sampling session over a melting pond.

The data collection process and subsequent laboratory analysis were designed to ensure the accuracy and reliability of the measurements. Samples were collected with a known-volume sampler, ensuring consistency. For each sample, the following parameters were recorded: resistance to penetration; grain size (in granular ice); time and coordinates. In laboratory, two methods were employed to estimate the density of the ice samples:
1. Mass and known volume: the sample was weighed using a balance scale. The volume of the sample was assumed to be the same as the known volume of the sampler.
2. Displacement method: the sample was placed in a graduated beaker filled with water; it was then submerged using a stick, and the increase in water volume was measured to determine the displaced volume of the sample. The sample was also weighed. For each sample, a descriptive sheet was compiled containing all the main information and images (Fig. 10).

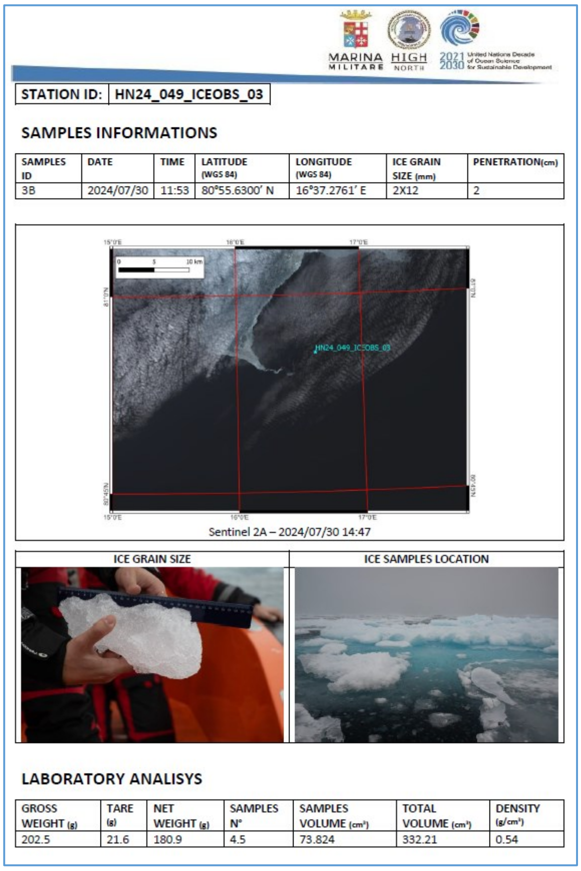

STATION ID: HN24_049_ICEOBS_03

SAMPLES INFORMATIONS

SAMPLES ID	DATE	TIME	LATITUDE (WGS 84)	LONGITUDE (WGS 84)	ICE GRAIN SIZE (mm)	PENETRATION(cm)
3B	2024/07/30	11:53	80°55.6300′ N	16°37.2761′ E	2X12	2

Sentinel 2A – 2024/07/30 14:47

ICE GRAIN SIZE | ICE SAMPLES LOCATION

LABORATORY ANALISYS

GROSS WEIGHT (g)	TARE (g)	NET WEIGHT (g)	SAMPLES N°	SAMPLES VOLUME (cm³)	TOTAL VOLUME (cm³)	DENSITY (g/cm³)
202.5	21.6	180.9	4.5	73.824	332.21	0.54

Fig. 10: Example of a sample description sheet.

F. *Estimating Ice Concentration from SAR Imagery*

One of the purposes of this study was to estimate sea ice concentration using Synthetic Aperture Radar (SAR) images obtained from Sentinel-1 and Cosmo-SkyMed satellites. In particular, 8 high-resolution multi-polarized images (with 2 or 4 polarizations) were acquired using Cosmo-SKYMed. Utilizing the HH polarization, which is particularly effective at distinguishing ice from open water, we aimed to develop a method for computing ice concentration over large oceanic areas, defined as the ratio of the pixel area covered by floating sea ice to the total area [13].

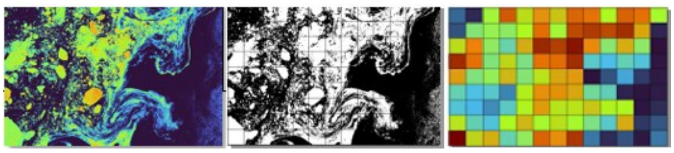

Fig.11A. Thresholding Radar Reflectivity; Fig. 11B: Grid Creation and Downscaling; Fig. 11C: Ice Concentration Calculation.

Moreover, using the four polarization bands of the COSMO-SkyMed satellite, we aimed at distinguishing between different types of ice and open ocean. We used various image processing and clustering techniques, with a focus on the Bisecting KMeans algorithm. This algorithm was selected after experimenting with other clustering techniques, as it proved most effective for our large dataset. Different numbers of clusters were tested to divide the dataset. In the initial phase of this research still in progress, the most representative result was the division into three clusters, which identified regions with a higher prevalence of water, scattered ice, and more compact ice. (Fig. 12) [14].

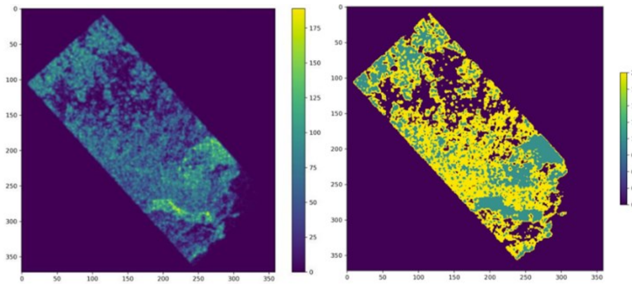

Fig.12. On the left, the multipolar image of a COSMO-SkyMed image, on the right, the result of clustering with 3 classes.

III. Results and Conclusions

At the conclusion of this interdisciplinary activity, the ability to process satellite images directly on-site allowed for synchronization of the ship's presence with the acquisition locations, allowing integration of remote sensing data with 22 in-situ samples and 4 UAV-based acquisitions, generating orthophotos and 3D photogrammetric reconstructions. Further time is needed to analyze the images and integrate them with laboratory data from the collected samples. Despite this, in this preliminary phase, successful concentration maps of ice presence were obtained, and a workflow for subsequent analyses was established. During the upcoming High North25 campaign next summer, satellite image acquisition and sampling activities will continue in order to gather a larger dataset for analysis.

Acknowledgment

Part of this work is carried out in the framework of a Phd in Civil, Chemical and Environmental Engineering on Remote Sensing for Oceanography with the University of Genoa (DICCA).

References

[1] Adams, S.; Willmes, S.; Heinemann, G.; Rozman, P.; Timmermann, R.; Schröder, D.; "Evaluation of simulated sea-ice concentrations from sea-ice/ocean models using satellite data and polynya classification methods."; Polar Research, Vol. 30(1), 2011.

[2] Kim, J.; Kim, D.; Hwang, B. P.; "Characterization of Arctic sea ice thickness using highresolution spaceborne polarimetric SAR data."; IEEE Transactions on Geoscience and Remote Sensing, Vol. 50(1), 13-22, 2012. [IC2]S. L Farrell, K. Duncan, K., E. Buckley, J. Richter - Menge, and R. Li, "Mapping sea ice surfacetopography in high fidelity with ICESat-2,". Geophysical Research Letters, 47, 2000.

[3] Mahmud, M. S.; Nandan, V.; Singha, S.; Howell, S. E. L.; Geldsetzer, T.; Yackel, J.; Montpetit, B.; "C- and L-band SAR signature of Arctic sea ice during freeze-up."; Remote Sensing of Environment, Vol. 279, 2022.

[4] Lyden, J. D.; Burns, B. A.; Maffett, A. L.; "Characterization of sea ice types using synthetic aperture radar."; IEEE Transactions on Geoscience and Remote Sensing, Vol. GE-22(5), 1984.

[5] Zakhvatkina, N. Y.; Smirnov, V.; Bychkova, I.; "Satellite SAR data-based sea ice classification: an overview". Geosciences, Vol. 9(4), Special Issue Cryosphere II, 2019.

[6] Asmus, V. V.; Vasilenko, E. V.; Zatyagalova, V. V.; Ivanova, N. P.; Krovotyntsev, V. A.; Maksimov, A. A.; Trenina, I. S.; "Satellite monitoring of sea ice cover and water parameters for the Caspian Sea."; Russian Meteorology and Hydrology, Vol. 43(10), 686-696, 2018.

[7] Dierking, W.; "Mapping of different sea ice regimes using images from Sentinel-1 and ALOS synthetic aperture radar."; IEEE Transactions on Geoscience and Remote Sensing, Vol. 48(3), 1045-1058, 2010.

[8] Johansson, A. M.; Brekke, C.; Spreen, G.; King, J. A.; "X-, C-, and L-band SAR signatures of newly formed sea ice in Arctic leads during winter and spring."; Remote Sensing of Environment, Vol. 204, 162-180, 2018.

[9] Li, Q.; Zhou, C.; Zheng, L.; Liu, T.; Yang, Z.; “Monitoring evolution of melt ponds on firstyear and multiyear sea ice in the Canadian Artic Archipelago with optical satellite data.”; Annals of Glaciology, Vol. 61(82), 2020.

[10] Dabboor, M.; Montpetit, B.; Howell, S.; Haas, C.; “Improving Sea Ice Characterization in dry ice winter conditions using polarimetric parameters from C- and L-band SAR data.”; Remote Sensing, Vol. 9(12), 1270-1287, 2017.

[11] Shokr, M.; Dabboor, M.; “Polarimetric SAR applications of sea ice: a review.”; IEEE Journal of Selected Topics in Applied Earth Observations and Remote Sensing, Vol.16, 1-16, 2023.

[12] Singha, S.; Johansson, M.; Hughes, N.; Hvidegaard, S. M.; Skourup, H.; “Arctic sea ice characterization using spaceborne fully polarimetric L-, C- and X- band SAR with validation by airborne measurements.”; IEEE Transactions on Geoscience and Remote Sensing, Vol. 56(7), 2018.

[13] Boulze, H.; Korosov, A. A.; Brajard, J.; “Classification of sea ice types in Sentinel-1 SAR data using convolutional neural networks.”; Remote Sensing, Vol. 12(13), Special Issue Polar Sea Ice: Detection, Monitoring and Modeling, 2020.

[14] Hillebrand, F. L.; Barreto, I. D. D. C.; Bremer, U. F.; Arigony-Neto, J.; Mendes Júnior, C. W.; Simões, J. C.; Da Rosa, C. N.; de Jesus, J. B.; “Application of textural analysis to map the sea ice concentration with Sentinel 1A in the western region of the Antarctic Peninsula.”; Polar Science, Vol. 29, 1-12, 2021.